Hindawi Publishing Corporation
Mathematical Problems in Engineering
Volume 2014, Article ID 972139, 12 pages
http://dx.doi.org/10.1155/2014/972139

Research Article

Energy Flow Chart-Based Energy Efficiency Analysis of a Range-Extended Electric Bus

Xiaogang Wu, Chen Hu, and Jingfu Chen

College of Electrical and Electronic Engineering, Harbin University of Science and Technology, Xue Fu Road 52, Harbin 150080, China

Correspondence should be addressed to Xiaogang Wu; xgwu@hrbust.edu.cn

Received 13 December 2013; Accepted 29 January 2014; Published 9 March 2014

Academic Editor: Hamid R. Karimi

This paper puts forward an energy flow chart analysis method for a range-extended electric bus. This method uses dissipation and cycle energy, recycle efficiency, and fuel-traction efficiency as evaluation indexes. In powertrain energy efficiency analysis, the range-extended electric bus is developed by Tsinghua University, the driving cycle based on that of Harbin, a northern Chinese city. The CD-CS and blended methods are applied in energy management strategies. Analysis results show with average daily range of 200 km, auxiliary power of 10 kW, CD-CS strategy, recycle ability and fuel-traction efficiency are higher. The input-recycled efficiency using the blended strategy is 24.73% higher than CD-CS strategy, while the output-recycled efficiency when using the blended strategy is 7.83% lower than CD-CS strategy.

1. Introduction

Compared with conventional fuel vehicles, application of electric vehicle decreases the dependency on petroleum and has the advantages of high energy efficiency and low environmental impact [1–3]. For a pure electric bus, the cost of a battery pack that can meet the driving range is too high; meanwhile, vehicle weight is too large for adding a large battery pack. A range-extended electric vehicle is regarded as one of the most suitable solutions for powertrain schemes, because of the maximum utility of the electric drive and the minimum capacity requirement of battery packs.

The main powertrain configurations of range-extended electric vehicles are series plug-in hybrid electric vehicles [4] and the Chevrolet Volt, produced by General Motors Corporation (GM) [5]. This paper will analyze a series plug-in hybrid electric bus.

In the studies of energy efficiency and fuel economy of range-extended electric vehicles, vehicle performance is analyzed on the basis of energy consumption and greenhouse gas emissions on the well-to-wheel and tank-to-wheel paths [6, 7]. Well-to-wheel fuel economy and greenhouse gas emissions data were obtained using the greenhouse gases, regulated emissions, and energy use in transportation (GREET) software model. The tank-to-wheel process is characterized by the recuperation and fuel-traction efficiencies, which are quantified and compared for two optimization-based energy management strategies.

The improvement of fuel economy for a range-extended electric vehicle can be realized by matching powertrain parts and a model selection method [8–12]. An optimal gen-set operating line method can minimize fuel consumption at a set level of electric output power. Series hybrid vehicles with direct injected stratified charge (DISC) rotary engines are proven to be more efficient in pure electric mode in terms of energy consumption and greenhouse gases (GHG) emissions than in vehicles with reciprocating engines.

Energy efficiency and fuel economy of range-extend electric vehicles can be improved by studying energy management strategy [13–16]. Researchers use dynamic programming strategies and equivalent consumption minimization strategies as well as Pontryagin's minimum principle strategy to analyze energy efficiency and fuel economy of range-extended electric vehicles, and results show that optimized energy management strategy can improve energy efficiency and fuel economy to a certain extent.

In conclusion, current studies on configuration analysis and energy management strategy on range-extended electric

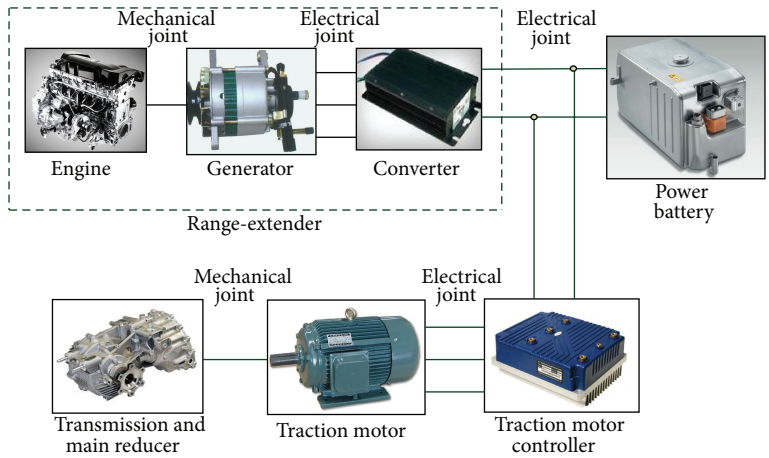

Figure 1: Powertrain configuration of the range-extended electric bus.

vehicles mainly focus on passenger vehicles, but work is rarely conducted into range-extended electric buses. Reference [17] asserts that a driving cycle significantly influences the energy efficiency and fuel economy of the vehicle. It proposes that construction and optimization of energy management strategy should consider different driving cycles. A system of energy efficiency analysis based on a certain driving cycle is the foundation of an optimal control strategy.

This paper focuses on the application requirements of the range-extended electric bus developed by Tsinghua University in Harbin and establishes the powertrain model of the bus based on the construction of the Harbin driving cycle. It examines the energy efficiency of the range-extended electric bus with two different energy management strategies (CD-CS and blended) and proposes improvement methods for energy efficiency.

2. Configuration and Principle of the Range-Extended Electric Bus

The range-extended electric vehicle lies between the plug-in hybrid electric vehicle and pure electric vehicle. Compared with a pure electric vehicle, a range-extended electric vehicle is supplemented with an onboard power generation system (range-extender) [18, 19]. The range-extender consists of engine, generator, and rectifier. The engine continually charges the power battery, so the driving range can be greatly increased to the level of a conventional internal combustion engine vehicle. The engine and power battery of a range-extended electric bus can be optimized at the same time. The working area of the engine can be optimized according to the driving cycle and the engine efficiency can be improved. The engine can operate with low pollution and fuel consumption. As for the battery, working condition of the power battery can also be optimized. If the power battery can continually work in good condition without overcharging or overdischarging, battery life can be extended. Braking energy can be recycled and energy consumption is decreased. The range-extender solves the problems of the energy consumption of air-conditioning, lighting, heating, and other electric auxiliaries, making the range-extended electric bus the most suitable solution for city buses.

A typical range-extended electric powertrain is shown in Figure 1. In a range-extended electric vehicle, wheels are driven directly by an electric motor. The motor draws energy from a battery pack and drives in pure electric mode when battery energy is available. Once the battery has been mostly depleted, the motor draws power from the range-extender, composed of an internal combustion engine and generator, in conjunction with a battery. Range-extended electric vehicles are designed with a predetermined all-electric range (AER). The AER represents the distance that the vehicle can travel using the energy stored in its battery only, without the engine and generator. Vehicles with a higher AER must have larger, heavier, and more expensive battery systems. The range-extended electric powertrain configuration is one of the most attractive applications for the diesel engine.

We can see the powertrain configuration of the range-extended electric bus discussed in this paper; the energy flow conditions of different driving modes are analyzed, as is shown in Figure 2. There are three driving modes: pure electric drive mode, range-extended mode, and regenerative brake mode.

Pure electric drive mode is shown in Figure 2(a). If SOC is high, the powertrain begins pure electric mode, whereby the engine stops and the motor will be driven by a power battery. Cheaper electric energy from the power grid is fully utilized. Fuel consumption and pollution are reduced in this mode. If SOC decreases to the set starting value, the range-extender begins and the powertrain works in range-extended mode.

Powertrain working in range-extended is shown in Figure 2(b). To increase driving range, if SOC decreases to the set starting value, the range-extender starts to generate power, reducing the rate of electricity loss and ensuring the motor can work to drive the bus. This mode can be divided into two kinds. One, if the output power of range-extender is lower than the motor required power, the lacking electric energy is provided by battery; the battery discharges. Two, if the output

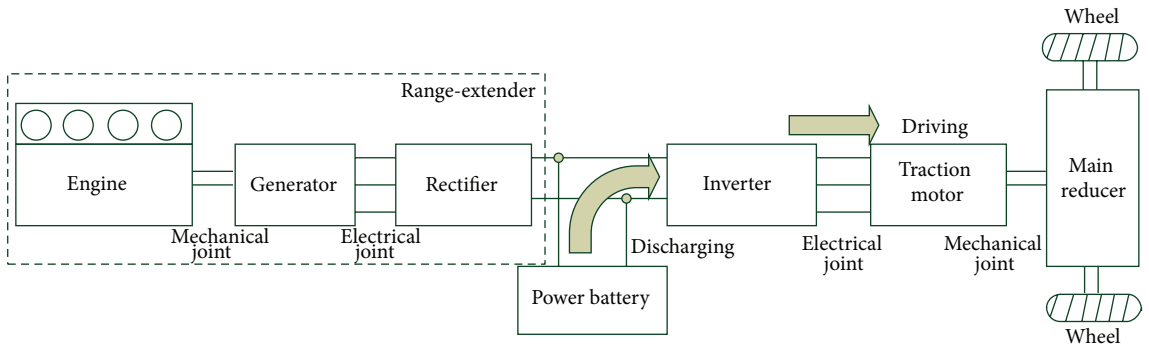

(a) Pure electric drive mode

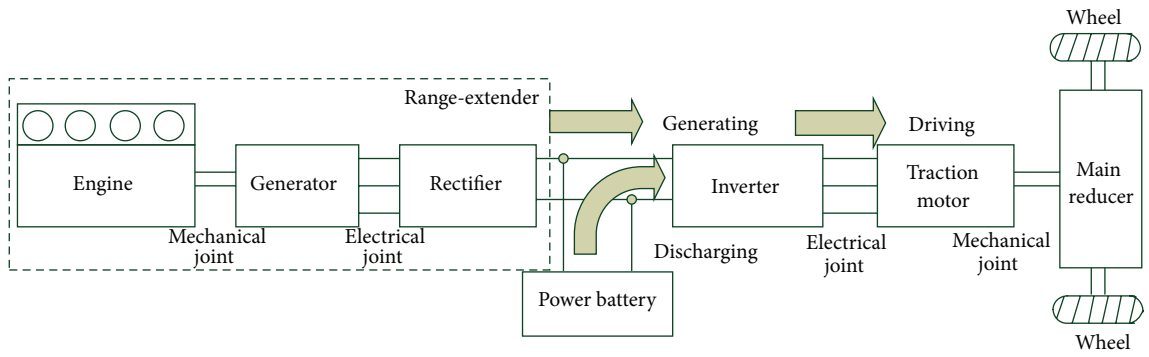

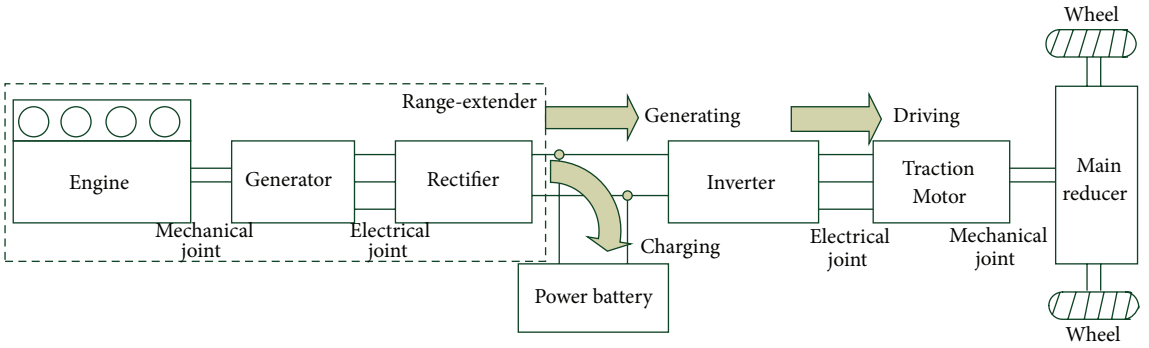

(b) Range-extended mode

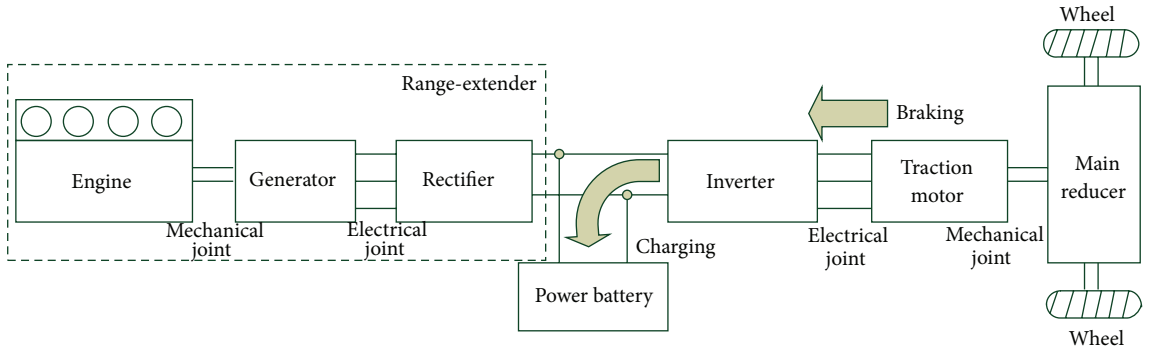

(c) Regenerative brake mode

Figure 2: Driving modes of the range-extended electric bus.

Figure 3: The range-extended electric bus developed by Tsinghua University.

power of the range-extender is higher than the required motor power, the redundant electric energy is reserved in battery, charging the battery. The output power of the range-extender is not directly influenced by the driving conditions and can be optimized in the high efficiency working areas of the engine and motor.

If the bus is braking, the motor can work in regenerative brake mode, as is shown in Figure 2(c). The motor provides braking torque for the vehicle wheels, and braking energy is transferred into electric energy reserved in the battery. Braking energy is not transferred into heat and lost; it is recycled.

For an individual axle drive bus, only wheels driven by the motor can recycle braking energy. Other wheels are stopped by mechanical braking. Braking energy is partly recycled and mechanical braking is also used on driven wheels for safety.

The range-extended electric bus analyzed in this paper is developed by Tsinghua University, shown in Figure 3. The powertrain is designed based on matching powertrain parts and model selection found in [20]. The generator is a permanent magnet generator and the traction motor is an asynchronous motor. Key parameters of the powertrain are listed in Table 1.

3. System Modeling of the Range-Extended Electric Bus

To analyze energy efficiency and fuel economy of the range-extended electric bus, system models based on benchmarks and modeling lines of [21–24] are built. The basic model of the range-extended electric system can be divided into four modules: range-extender module, traction motor module, power battery module, and the vehicle longitudinal dynamics module. Considering the high complexity of a diesel engine, permanent magnet synchronous generator, and the rectifier and driving motor, relevant components are tested by benchmarks and the characteristics MAP are determined according to the test results. Then, the simulation models are built based on the MAP, which replaces the complex mathematical description, reduces modeling complexity, and therefore improves model credibility.

Table 1: Powertrain parameters of range-extended electric bus.

Vehicle	Size (length × width × height)/mm	11980 × 2550 × 3200
	Vehicle mass/kg	13000
	Rated passengers	78
	Windward area/m^2	7.5
	Air resistance coefficient C_D	0.75
	Rolling resistance coefficient f	$0.0076 + 0.00056u_a$
	Rolling radius r/m	0.512
	Speed ratio of main reducer i_0	6.2
	Speed ratio of transmission i_g	2.34
Motor	Continuous power/kW	100
	Peak power/kW	180
	Maximum torque/N·m	860
	Maximum speed/r/min	4500
	Operating voltage/V	300~450
Engine	Displacement/L	1.9
	Power/kW	82/4000 r/min
Generator	Rated power/kW	50
	Rated torque/N·m	220
Power Battery	Capacity	180 Ah
	Operating voltage/V	350~460

3.1. Range-Extender. The range-extender includes a diesel engine, a permanent magnet synchronous generator, and rectifier. System features can be described by the following equations:

$$\begin{aligned} n_{\text{eng}} &= n_r \frac{1}{\tau_e s + 1}, \\ T_{\text{eng}} &= f_1\left(\alpha, n_{\text{eng}}\right), \\ C_{\text{eng}} &= f_2\left(n_{\text{eng}}, T_{\text{eng}}\right), \\ \eta_{\text{gr}} &= f_3\left(n_{\text{eng}}, \lambda\right) \cdot \eta_r, \end{aligned} \tag{1}$$

where f_1 is the accelerator characteristic MAP of the engine, f_2 is fuel consumption characteristic MAP of the engine, f_3 is the generator efficiency MAP, n_r is the engine's target speed, ζ_e is a time constant, α is the accelerator signal, n_{eng} is the engine's actual speed, T_{eng} is the engine torque, λ is the generator loading rate, η_r is the rectifier efficiency, C_{eng} is the engine's instantaneous fuel consumption, and η_{gr} is the total rate of the generator and rectifier.

3.2. Traction Motor. The traction motor module includes the motor and motor controller. The motor model consists of the

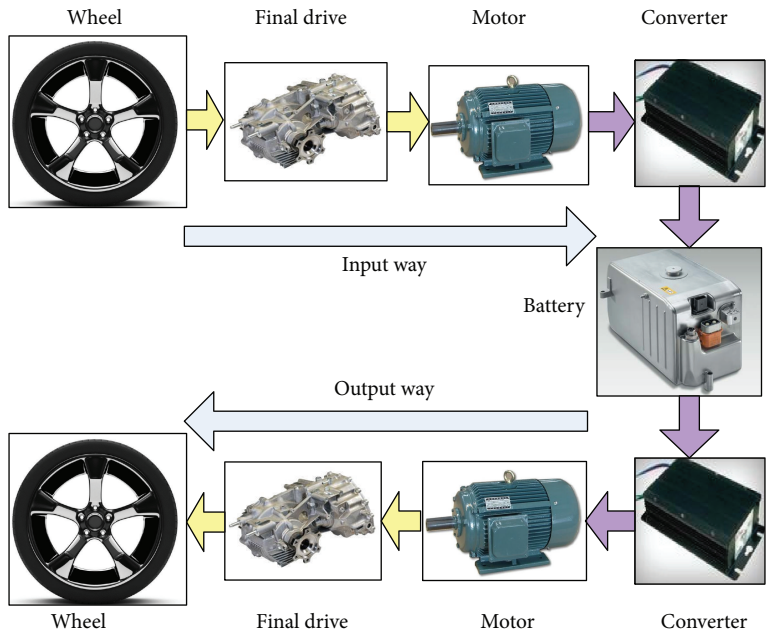

Figure 4: Schema of recycle energy flow.

steady state efficiency characteristic MAP and a first-order process:

$$\eta_m = f_{m1}(n_m, T_m),$$
$$T_m = \min(T_r, T_{\max}) \cdot \frac{1}{\tau_m s + 1}, \quad (2)$$
$$T_{\max} = f_{m2}(n_m),$$

where η_m is the motor's electric efficiency, n_m is the motor's rotational speed, ζ_m is a time constant, and T_m, T_r, and $T_{\max}$ are the motor's actual torque, target torque, and torque capacity, respectively. The function f_{m1} denotes the motor's efficiency MAP, and f_{m2} denotes the motor's maximum output torque characteristic MAP.

3.3. Power Battery. The power battery model is built based on the R_{int} model, which is equivalent to a variable voltage source and a variable resistance in series. According to the battery internal resistance equivalent circuit, the following equation can be established:

$$U_{\text{oc}} = E(\text{SOC}, T) - I \cdot R(\text{SOC}, T), \quad (3)$$

where SOC is the state of charge of the battery, T is the temperature, and I is the battery current. E stands for the open circuit voltage of the battery, which is a function of SOC, T is determined by the test, and R is the internal resistance of the battery.

In this model, the battery's SOC state uses ampere-hour integral method to estimate [25]. That is, when the vehicle is in operation, it will use SOC as SOC_{int} and at t moment it will use SOC formula (4) to decide the following:

$$\text{SOC} = \text{SOC}_{\text{int}} - \frac{1}{Q_b}\int_{t_0}^{t} \eta_{\text{bat}} I_{\text{bat}}\, dt, \quad (4)$$

where Q_b is rated capacity, η_{bat} is the battery's columbic capacity, and I_{bat} is its charging and discharging current.

3.4. Vehicle Longitudinal Dynamics. The road load characteristic is assumed to be ideal in simulation, that is, zero air speed and good adhesion. As the vehicle is traveling on the road, traction motor needs to overcome driving resistance (F_t), rolling resistance (F_f), air resistance (F_w), slope resistance (F_i), and acceleration resistance (F_j). Consider

$$F_t = F_f + F_w + F_i + F_j,$$
$$F_f = fmg\cos(a\tan i),$$
$$F_w = \frac{1}{2}C_d A\rho u_a^2,$$
$$F_i = mg\sin(a\tan i), \quad (5)$$
$$F_j = 0.28\delta m\frac{du_a}{dt},$$
$$F_t = \frac{3.6\eta_T P_{\text{motor}}}{u_a},$$

where f is the rolling resistance coefficient, m is the vehicle mass, g is the acceleration of gravity, i is the road slope, C_d is the coefficient of air resistance, A is the windward area, ρ is the air density, u_a is the motor speed, δ is the correction coefficient of rotating mass, η_T is the overall efficiency of drive system, and P_{motor} is the output power of the traction motor.

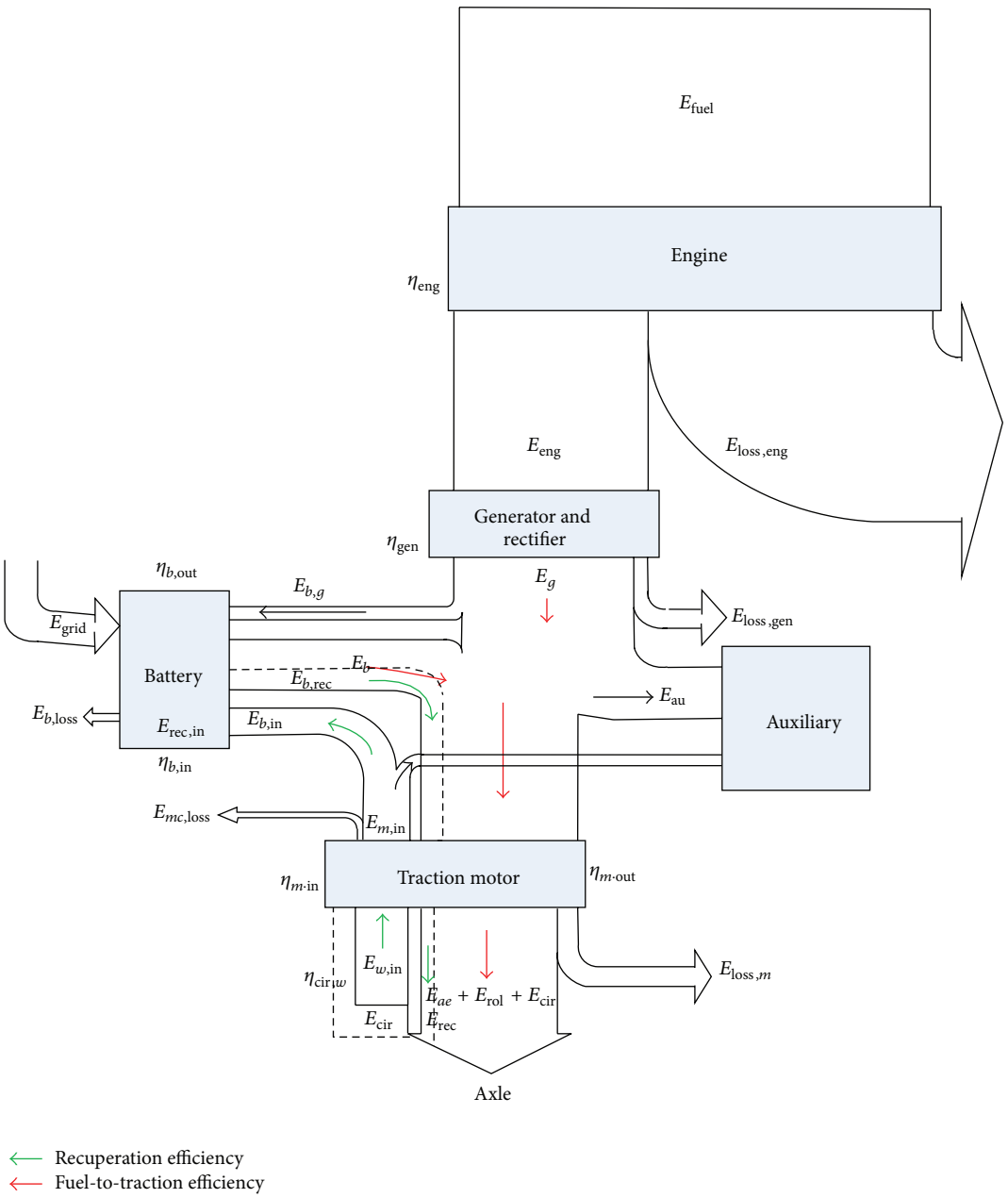

FIGURE 5: Energy flow chart in energy efficiency analysis.

4. Energy Efficiency Analysis Using Energy Flow Chart

According to the energy efficiency analysis method of plug-in hybrid electric powertrain in [7], energy efficiency analysis can be divided into the following three parts.

4.1. Dissipation and Cycle Energy. Traction power is used to drive the wheels and vehicle auxiliaries; the calculation equation is as follows:

$$P(t) = P_{ae}(t) + P_{rol}(t) + P_{au}(t) + P_{ac}(t) + P_{gr}(t), \quad (6)$$

where $P_{ae}(t) = \rho_{air} A_f c_d v^3(t)/2$ is the power to overcome air resistance, ρ_{air} is the air density, A_f is the frontal area, c_d is the air resistance coefficient, v is the vehicle speed, $P_{rol}(t) = (m_v + m_p) g c_r \cos(\alpha(t)) v(t)$ is the power to overcome rolling resistance, $P_{ac}(t) = (m_v + m_p) v(t) v(t) (dv(t)/dt)$ is the acceleration/deceleration power, $P_{gr}(t) = (m_v + m_p) g \sin(\alpha(t)) v(t)$ is the up/down hill power, v is the vehicle speed, α is the road gradient, m_p is the battery mass, and $P_{au}(t)$ is the auxiliaries power, including air condition, battery heat management system, heating (seat heating and windshield heating), lighting, control system, and braking steer consumption. The average power of the auxiliaries is 10 kW [26], assuming air-conditioning is working.

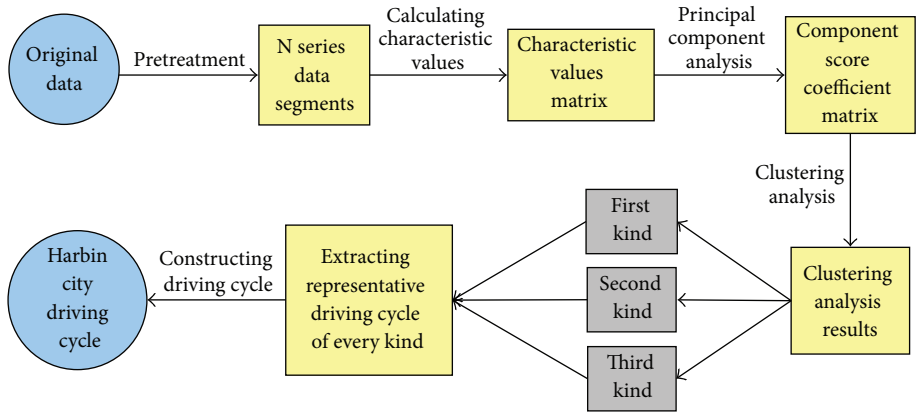

Figure 6: Construction process of Harbin city driving cycle.

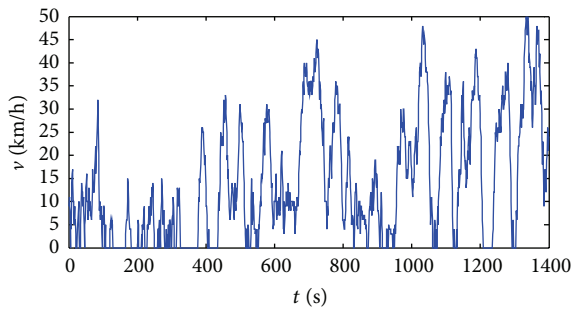

Figure 7: Harbin city driving cycle.

$P(t)$ can be divided into two parts: one is the dissipated power $P_{\text{dis}}(t) = P_{\text{ae}}(t) + P_{\text{rol}}(t) + P_{\text{au}}(t)$ and the other is conserved power $P_{\text{cons}}(t) = P_{\text{ac}}(t) + P_{\text{gr}}(t)$. As the initial and final altitude and speed are the same in a whole driving cycle, the reserved power is zero. If braking energy can be fully recycled, required traction energy E_{trac} should be the same as the dissipated energy E_{dis}

$$E_{\text{trac}} = \int_{t_0}^{t_f} P(t)\,dt = \int_{t_0}^{t_f} P_{\text{dis}}(t)\,dt = E_{\text{dis}}, \tag{7}$$

where t_0 and t_f are initial and final time. If there is no barking energy recycled,

$$\begin{aligned} E_{\text{trac}} &= \int_{P(t)>0} P(t)\,dt \\ &= \int_{t_0}^{t_f} P_{\text{dis}}(t)\,dt + \int_{P(t)<0} (-P(t))\,dt \\ &= E_{\text{dis}} + \int_{P(t)<0} (-P(t))\,dt, \end{aligned} \tag{8}$$

where $\int_{P(t)<0}(-P(t))dt$ represents the cycle energy E_{cir}, which is the temporal vehicle cycle energy in the form of kinetic or potential energy and ultimately dissipated during friction braking. Therefore, (8) for vehicle without energy recycle can be calculated as

$$E_{\text{trac}} = E_{\text{dis}} + E_{\text{cir}}. \tag{9}$$

In actual driving, energy balance equation can be calculated as

$$E_{\text{trac}} = E_{\text{dis}} + E_{\text{cir}} - E_{\text{rec}}, \tag{10}$$

where E_{rec} is the recycled net energy that is usable for traction. According to (7) and (10), it can be found that $E_{\text{rec}} = E_{\text{cir}}$.

4.2. Recycle Efficiency of Barking Energy. Recycle efficiency is defined as

$$\eta_{\text{rec}} = \frac{E_{\text{rec}}}{E_{\text{cir}}}. \tag{11}$$

As E_{cir} can be easily obtained in driving cycle, the key mission is to calculate E_{rec}. Recycle energy consists of two flow methods: input and output. As is shown in Figure 4, recycle ability is determined by energy dissipation, motor torque, current of power battery, and threshold charge value.

Time set S is defined as

$$S = \left\{ t \mid t \in \left[t_0, t_f\right], P(t) - P_{\text{au}}(t) < 0, P_b(t) < 0 \right\}, \tag{12}$$

where P_{au} is physical load in converter. $E_{w,\text{in}}$ is absolute input energy during S and is calculated by

$$E_{w,\text{in}} = \int_S \left| P(t) - P_{\text{au}}(t) \right| dt. \tag{13}$$

The energy reserved in battery is

$$E_{b,\text{in}} = \int_S \left| P_b(t) + I(t)^2 R n_c \right| dt. \tag{14}$$

The energy loss is

$$E_{\text{loss,in}} = E_{w,\text{in}} - E_{b,\text{in}} - \int_S P_{\text{au}}(t)\,dt. \tag{15}$$

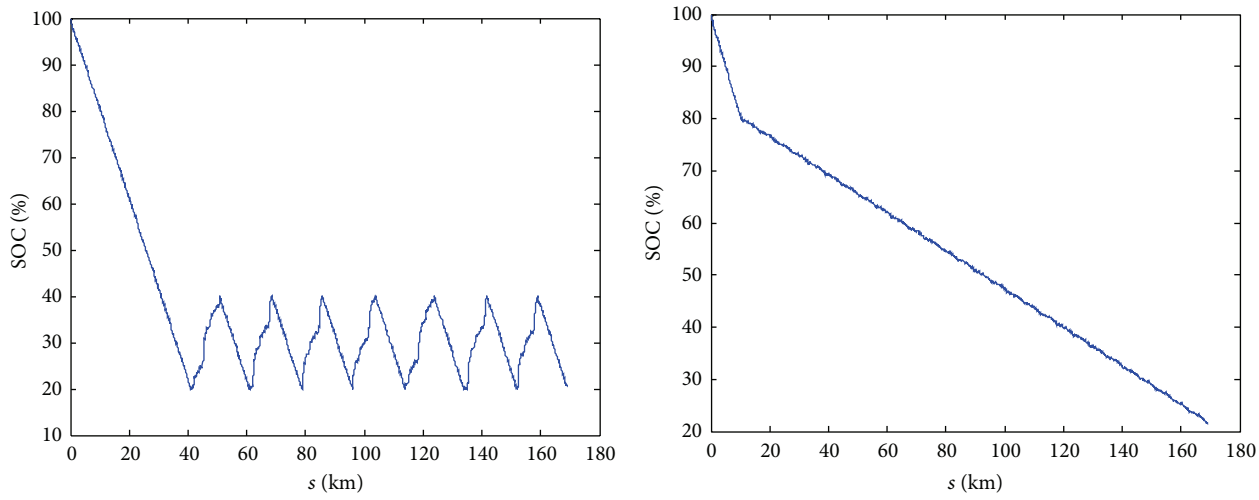

(a) CD-CS strategy (b) Blended strategy

FIGURE 8: The SOC curve with the two different energy management strategies.

The cycle-average wheel to battery energy efficiency is

$$\eta_{\text{wb, in}} = 1 - \frac{E_{\text{loss, in}}}{E_{w, \text{in}}}. \tag{16}$$

The recycle energy reserved in battery is

$$E_{\text{rec, in}} = E_{\text{cir}} \eta_{\text{wb, in}} \eta_{\text{cir}, w}, \tag{17}$$

where $\eta_{\text{cir}, w}$ is the ratio between E_w and E_{cir}.

Time set D is defined as

$$D = \left\{ t \mid t \in \left[t_0, t_f \right], P(t) - P_{\text{au}}(t) \geq 0, P_b(t) \geq 0 \right\}. \tag{18}$$

The associated motor energy loss in propelling is

$$E_{\text{loss}, m} = \int_D P_{\text{loss}, m}(t)\, dt. \tag{19}$$

The average motor efficiency is

$$\eta_{m, \text{out}} = 1 - \frac{E_{\text{loss}, m} d}{\int_D P_b(t) \eta_{\text{con}} + P_{\text{apu}}(t) \eta_{\text{con}} - P_{\text{au}}(t)\, dt}. \tag{20}$$

The battery energy loss during time D is

$$E_{\text{loss}, b} = \int_D I(t)^2 R n_c dt. \tag{21}$$

The battery efficiency in output way is

$$\eta_{b, \text{out}} = 1 - \frac{E_{\text{loss}, b} d}{\int_D P_b(t) + I(t)^2 R n_b\, dt}. \tag{22}$$

The cycle-average battery to wheel energy efficiency is

$$\eta_{\text{bw, out}} = \eta_{b, \text{out}} \eta_{\text{con}} \eta_{m, \text{out}} \eta_{fd} \eta_{b, m}, \tag{23}$$

where $\eta_{b, m}$ is the ratio between the power that battery provides to the motor and the power emitted by battery. According to (16) and (23), the recycle energy for traction is

$$E_{\text{rec}} = E_{\text{rec, in}} \eta_{\text{bw, out}}. \tag{24}$$

The cycle-average recycle efficiency is

$$\eta_{\text{rec}} = \frac{E_{\text{rec}}}{E_{\text{cir}}} = \eta_{\text{cir}, w} \eta_{\text{wb, in}} \eta_{\text{bw, out}}. \tag{25}$$

4.3. Fuel-Traction Efficiency. Fuel-traction efficiency is defined as

$$\eta_{\text{ft}} = \frac{E_{\text{trac}}}{E_{\text{ef}}} = \frac{E_{\text{dis}} + (1 - \eta_{\text{rec}}) E_{\text{cir}}}{E_{\text{ef}}}, \tag{26}$$

where E_{ef} is the equal fuel energy, the average consumption of the sum of diesel, and electric energy. η_{ft} is the cycle-average conversion efficiency from the total consumed energy to the mechanical energy at the wheels and the electrical energy for the auxiliaries. Based on the initial and final SOC, E_{ef} can be divided into diesel energy and electric energy.

An energy flow chart can clearly show the direction of energy flow, showing the sizes of losses from each individual part. It is one of the most effective methods for analyzing flow in the context of system performance. Referring to the analysis method in [27], this paper puts forward a powertrain energy analysis method with energy flow chart for range-extended electric bus. The powertrain energy flow chart is shown in Figure 5.

5. Analysis Example with the Driving Cycle of Harbin City

To provide a credible reference for the match and control of the range-extended electric bus, energy efficiency analysis

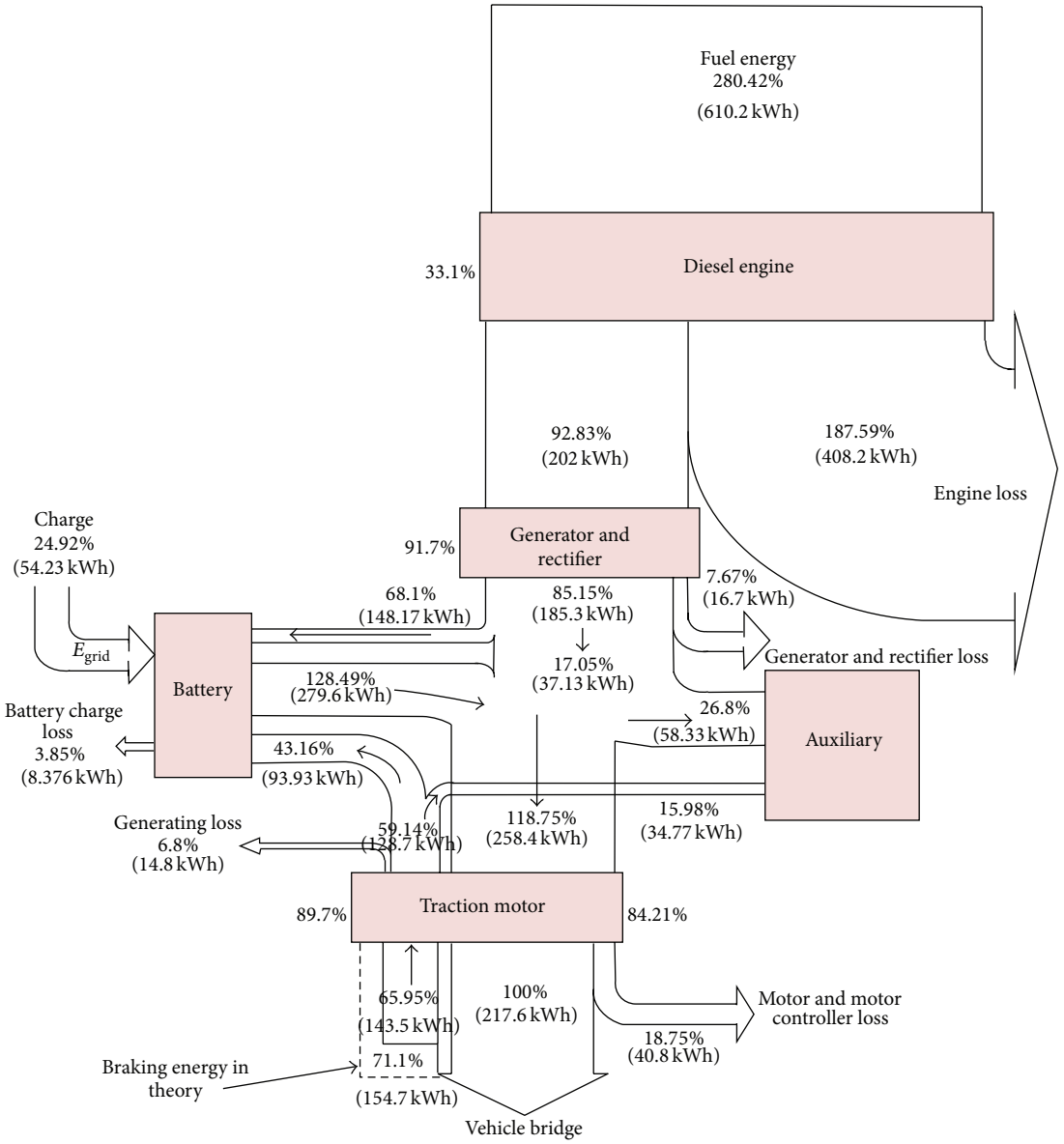

Figure 9: Energy flow chart with CD-CS strategy.

should be carried out within a driving cycle. Based on the authors' location, the Harbin city driving cycle has been chosen for this paper, and the construction process is shown in Figure 6.

The constructed Harbin city driving cycle is shown in Figure 7; acceleration and deceleration are frequent. The maximum acceleration is 1.94 m/s^2, the idle proportion is 22.3%, the maximum speed is 50 km/h, and the average speed is 14.5 km/h.

The analysis process mainly compares the CD-CS strategy with the switching control method on the range-extender and blended strategy with power following control method on the range-extender. According to the research, the daily average range for Harbin city bus line 101 is 150–180 km, the initial SOC is 100%, and the auxiliaries' power is 10 kW. SOC curves with the two different driving cycles are shown in Figure 8.

Figure 9 shows the energy flow chart with CD-CS strategy, and Figure 10 shows the energy flow chart with blended strategy.

Based on Figure 5, the input and output recycle efficiencies can be obtained, as is shown in Figure 11. The input-recycled efficiency of the blended strategy is 24.73% higher than that of CD-CS strategy. The output-recycled efficiency of the blended strategy is 7.83% lower than that of the CD-CS strategy.

Figure 12 consists of recycle efficiency, fuel-traction efficiency, and energy consumption with the two different energy management strategies. As is shown in Figure 12(a), the recycle efficiency is 36.80% with CD-CS strategy and 51.32% with blended strategy. With CD-CS strategy, the fuel-traction efficiency is 38.91%, but, with blended strategy, it is 33.26%. The fuel-traction efficiency is limited by engine efficiency and

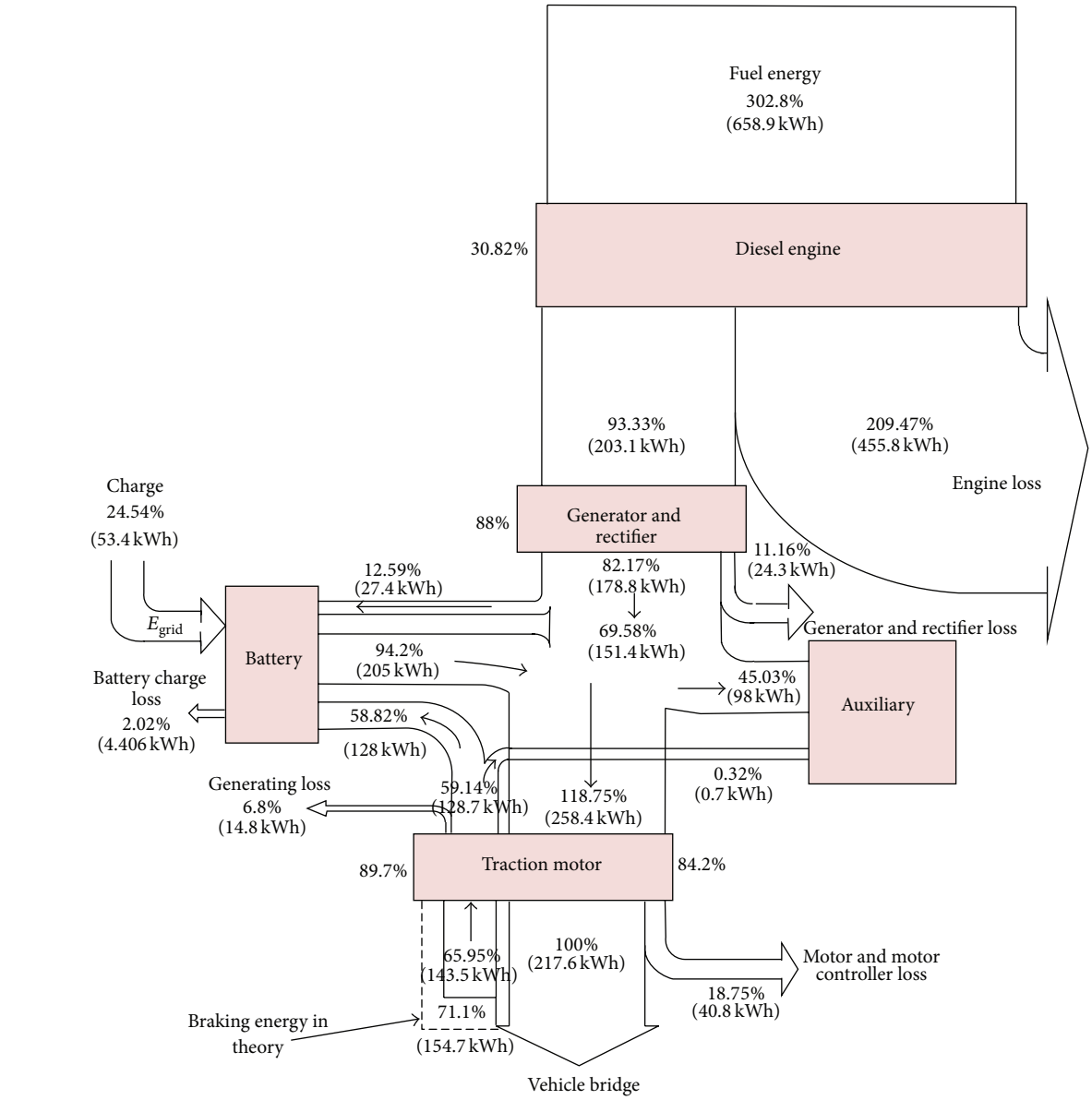

Figure 10: Energy flow chart with blended strategy.

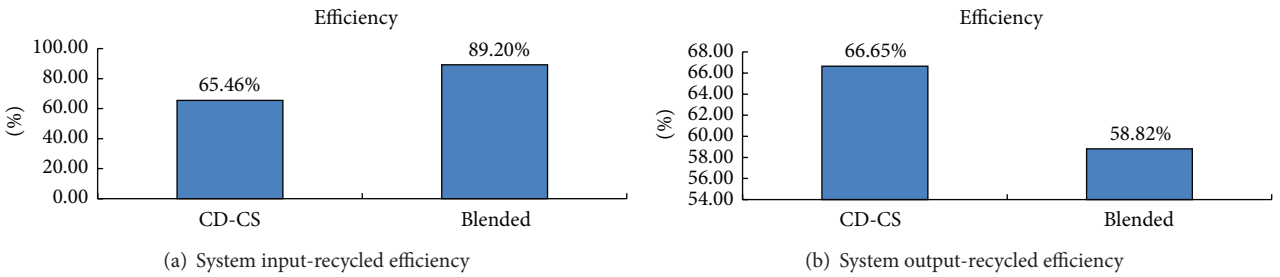

(a) System input-recycled efficiency

(b) System output-recycled efficiency

Figure 11: Comparison of powertrain input- and output-recycled efficiency with different energy management strategies.

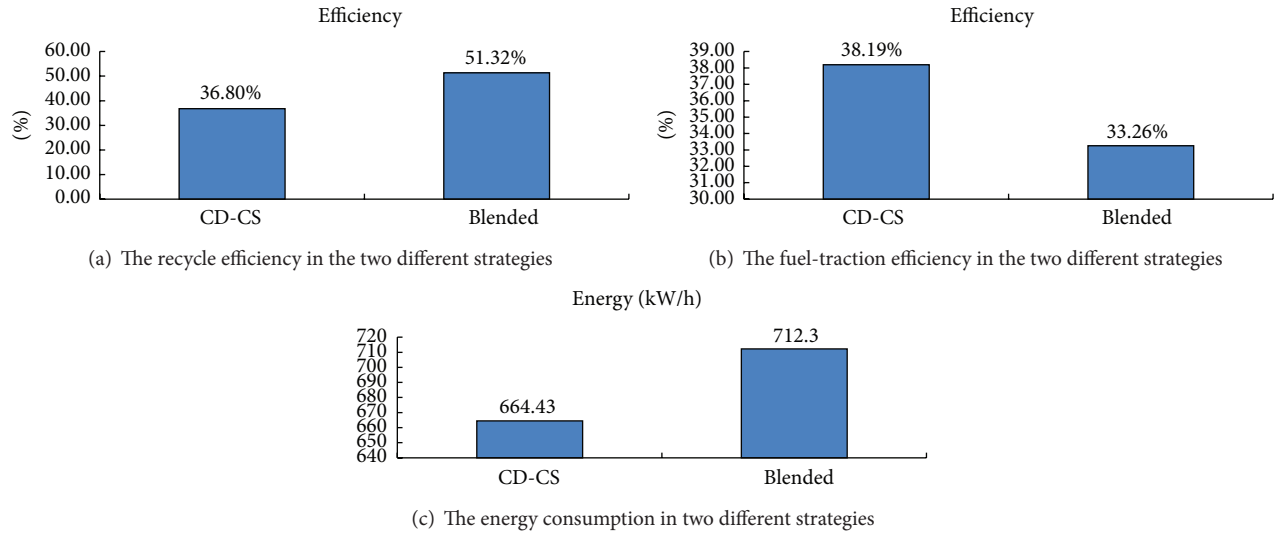

(a) The recycle efficiency in the two different strategies

(b) The fuel-traction efficiency in the two different strategies

(c) The energy consumption in two different strategies

Figure 12: Comparison of recycle efficiency, fuel-traction efficiency, and energy consumption with different energy management strategies.

is also influenced by other electric and mechanical losses, such as the battery, power converter, and motor and drive system. Energy consumption is 664.43 kWh with the CD-CS strategy and 47.87 kWh lower than that with the blended strategy. The CD-CS strategy has a better recycle ability and fuel-traction efficiency. It is worth noting that the yearly range of one bus in Harbin is nearly 70000 km, and the energy saved with the CD-CS strategy would be considerable.

6. Conclusions

For a range-extended electric bus developed by Tsinghua University, this paper analyzes the energy efficiency with two different energy management strategies (CD-CS and blended) using an energy flow chart method. Harbin city driving cycle is taken for analysis. The recycle efficiency and fuel-traction efficiency are evaluation indexes.

Analysis results from the energy flow chart show that the energy loss mainly occurs at the engine. Engine energy loss reaches 187.59% of the whole driving energy using the CD-CS strategy and 209.47% with the blended strategy. As the CD-CS strategy uses a thermostat control method, its charging loss is 3.85% of total driving energy, while the blended strategy only has a 2% charging loss. Of these two energy management strategies, the CD-CS strategy can effectively reduce the engine loss but has a higher charging loss compared with the blended strategy.

Energy efficiency results show that over the Harbin city driving cycle, the input-recycled efficiency of the blended strategy is 24.73% higher than that of the CD-CS strategy and that the output-recycled efficiency of the blended strategy is 7.83% lower than that of the CD-CS strategy. With the CD-CS strategy, the recycle efficiency is 36.80%, but, with blended strategy, it is 51.32%. Using the CD-CS strategy, the fuel-traction efficiency is 38.91%, but, with blended strategy, it is 33.26%. In comparison of the two nonoptimized energy management strategies, powertrain energy efficiency is better with CD-CS than with blended strategy. We suggest that a CD-CS energy management strategy is more appropriate for the driving conditions on urban Harbin roads.

Conflict of Interests

The authors declare that there is no conflict of interests regarding the publication of this paper.

Acknowledgment

This work is supported by the National Natural Science Foundation (NNSF) of China (Grant no. 51105220).

References

[1] G. Wang, "Advanced vehicles: costs, energy use, and macroeconomic impacts," *Journal of Power Sources*, vol. 196, no. 1, pp. 530–540, 2011.

[2] P. Baptista, M. Tomás, and C. Silva, "Plug-in hybrid fuel cell vehicles market penetration scenarios," *International Journal of Hydrogen Energy*, vol. 35, no. 18, pp. 10024–10030, 2010.

[3] H. Li, X. Jing, and H. R. Karimi, "Output-feedback based H_∞ control for active suspension systems with control delay," *IEEE Transactions on Industrial Electronics*, vol. 61, no. 1, pp. 436–446, 2014.

[4] T.-W. Chun, Q.-V. Tran, H.-H. Lee, H.-G. Kim, and E.-C. Nho, "Simulator for monitoring the operations of range extender electric vehicles," *Journal of Power Electronics*, vol. 11, no. 4, pp. 424–429, 2011.

[5] R. Matthe, L. Turner, and H. Mettlach, "VOLTEC battery system for electric vehicle with extended range," *SAE International Journal of Engines*, vol. 4, no. 1, pp. 1944–1962, 2011.

[6] S. Varnhagen, A. Same, J. Remillard, and J. W. Park, "A numerical investigation on the efficiency of range extending systems using advanced vehicle simulator," *Journal of Power Sources*, vol. 196, no. 6, pp. 3360–3370, 2011.

[7] X. Hu, N. Murgovski, L. Johannesson, and B. Egardt, "Energy efficiency analysis of a series plug-in hybrid electric bus with different energy management strategies and battery sizes," *Applied Energy*, vol. 111, pp. 1001–1009, 2013.

[8] D. H. Lee, N. W. Kim, and J. R. Jeong, "Component sizing and engine optimal operation line analysis for a plug-in hybrid electric transit bus," *International Journal of Automotive Technology*, vol. 14, no. 3, pp. 459–469, 2013.

[9] S. Varnhagen, A. Same, J. Remillard, and J. W. Park, "A numerical investigation on the efficiency of range extending systems using Advanced Vehicle Simulator," *Journal of Power Sources*, vol. 196, no. 6, pp. 3360–3370, 2011.

[10] M. Masih-Tehrani, M.-R. Ha'iri-Yazdi, V. Esfahanian, and H. Sagha, "Development of a hybrid energy storage sizing algorithm associated with the evaluation of power management in different driving cycles," *Journal of Mechanical Science and Technology*, vol. 26, no. 12, pp. 4149–4159, 2012.

[11] J. Waldner, J. Wise, C. Crawford, and Z. Dong, "Development and testing of an advanced extended range electric vehicle," SAE 2011-01-0913, 2011.

[12] A. M. Joshi, H. Ezzat, N. Bucknor, and M. Verbrugge, "Optimizing battery sizing and vehicle lightweighting for an extended range electric vehicle," SAE 2011-01-1078, 2011.

[13] M. Cipek, M. Coric, B. Skugor, J. Kasac, and J. Deur, "Dynamic programming-based optimization of control variables of an extended range electric vehicle," SAE 2013-01-1481, 2013.

[14] B. Skugor and J. Deur, "Instantaneoun optimization-based energy management control strategy for extended range electric vehicle," SAE 2013-01-1460, 2013.

[15] L. Xu, F. Yang, and M. Hu, "Comparison of energy management strategies for a range extended electric city bus," *Journal of University of Science and Technology of China*, vol. 42, no. 8, pp. 640–647, 2012.

[16] C. Hou, M. Ouyang, and L. Xu, "Approximate Pontryagin's minimum principle applied to the energy management of plug-in hybrid electric vehicles," *Journal of Applied Energy*, vol. 115, pp. 174–189, 2014.

[17] X. Wu, J. Du, and C. Hu, "Energy efficiency and fuel economy analysis of a series hybrid electric bus in different Chinese city driving cycles," *International Journal of Smart Home*, vol. 7, no. 5, pp. 353–368, 2013.

[18] E. D. Tate, O. H. Michael, and J. S. Peter, "The electrification of the automobile: from conventional hybrid, to plug-in hybrids, to extended-range electric vehicles," SAE 2008-01-0458, 2008.

[19] K. Dominik, P. Sylvain, and K. Jason, "'Fair' comparison of powertrain configurations for plug-in hybrid operation using global optimization," SAE 2009-01-1334, 2009.

[20] X. Wu and L. Lu, "System matching and simulation of a plug-in series hybrid electric vehicle," *Automotive Engineering*, vol. 35, no. 7, pp. 573–582, 2013.

[21] H.-S. Xiong, G.-J. Cao, L.-G. Lu, M.-G. Ouyang, and J.-Q. Li, "Simulation system of series hybrid powertrain for city bus and its applications," *Journal of System Simulation*, vol. 22, no. 5, pp. 1134–1138, 2010.

[22] Q. Yang, J. Huang, G. Wang, and H. Reza Karimi, "An adaptive metamodel-based optimization approach for vehicle suspension system design," *Mathematical Problems in Engineering*, vol. 2014, Article ID 965157, 9 pages, 2014.

[23] J. Rubió-Massegú, F. Palacios-Quiñonero, J. M. Rossell, and H. Reza Karimi, "Static output-feedback control for vehicle suspensions: a single-step linear matrix inequality approach," *Mathematical Problems in Engineering*, vol. 2013, Article ID 907056, 12 pages, 2013.

[24] Q. Lu, H. Reza Karimi, and K. Gunnar Robbersmyr, "A data-based approach for modeling and analysis of vehicle collision by LPV-ARMAX models," *Journal of Applied Mathematics*, vol. 2013, Article ID 452391, 9 pages, 2013.

[25] Z. Li, L. Lu, and M. Ouyang, "Comparison of methods for improving SOC estimation accuracy through an ampere-hour integeration approach," *Journal of Tsinghua University*, vol. 50, no. 8, pp. 1293–1301, 2010.

[26] J. Campbell, W. Watts, and D. Kittelson, "Reduction of accessory overdrive and parasitic loading on a parallel electric hybrid city bus," SAE 2012-01-1005, 2012.

[27] S. Campanari, G. Manzolini, and F. Garcia de la Iglesia, "Energy analysis of electric vehicles using batteries or fuel cells through well-to-wheel driving cycle simulations," *Journal of Power Sources*, vol. 186, no. 2, pp. 464–477, 2009.